AJNR

Imaging of normal leptomeningeal melanin.

S S Gebarski and M A Blaivas

AJNR Am J Neuroradiol 1996, 17 (1) 55-60
http://www.ajnr.org/content/17/1/55

This information is current as
of October 11, 2024.

Imaging of Normal Leptomeningeal Melanin

Stephen S. Gebarski and Mila A. Blaivas

PURPOSE: To find the CT and MR characteristics of normal leptomeningeal melanin, which can be macroscopically visible at autopsy in decedents with deeply pigmented skin. **METHODS:** For the normal anatomic study, there were two black subjects who had had brain MR and CT within 12 months before autopsy that showed leptomeningeal melanin. For the normal imaging study, brain MR was done on 74 patients (31 black), and CT in 24 of these 74 patients. **RESULTS:** In the normal anatomic study, the pattern of T2-weighted hypointensities on the surface of the medulla oblongata matched the histopathologic distribution of leptomeningeal melanin. A similar signal was seen in 28 of the 31 black patients in the normal imaging study. Such a signal was subtle, or entirely absent, in the other patients. CT showed no reliable altered attenuation corresponding to the histopathologic distribution of leptomeningeal melanin. **CONCLUSION:** Normal leptomeningeal melanin is visible on MR as T2-weighted hypointensities along the surface of the medulla oblongata. The signal changes can be profound and might simulate leptomeningeal diseases that contain melanin or iron. This normal pigmentation should be taken into account before diagnosing abnormalities in this region.

Index terms: Meninges, magnetic resonance; Meninges, computed tomography

AJNR Am J Neuroradiol 17:55–60, January 1996

Melanocytes are normally found in the leptomeninges, the number generally being proportional to skin pigmentation (1–4). The density of these cells increases markedly in the leptomeninges of the medulla oblongata and upper cervical cord, where such pigmentation can be visible to the naked eye on autopsy (1–4). Magnetic resonance (MR) imaging signal changes attributable to melanin are variable but can be profound (5–7). Computed tomographic (CT) and MR imaging findings in meningeal diseases, including melanin-containing entities, have been reported (7–11). We designed a retrospective study to find the CT and MR imaging characteristics of normal leptomeningeal melanin.

Received March 29, 1995; accepted after revision June 20.

From the Departments of Radiology (S.S.G.) and Pathology (M.A.B.), University of Michigan Medical School, Ann Arbor.

Address reprint requests to Stephen S. Gebarski, MD, Department of Radiology/B1D530, University Hospital, 1500 E Medical Center Dr, Ann Arbor, MI 48109-0030.

AJNR 17:55–60, Jan 1996 0195-6108/96/1701–0055
© American Society of Neuroradiology

Patients and Methods

Our study consisted of two parts. First, the normal anatomic study was an imaging and pathologic correlation using premorbid imaging and autopsy material. Second, the normal imaging study was a review of the clinical records and imaging in patients with normal brain CT and/or MR imaging.

Normal Anatomic Study

Autopsy and MR imaging records were searched to find black persons who had premorbid CT and MR imaging focused on the posterior fossa. Patients were selected if they had this imaging within 12 months before autopsy, which included examination of the brain. The stored brain tissue was reviewed for the presence of leptomeningeal melanin, selecting only those persons with leptomeningeal melanin visible to the naked eye. The brain tissue of these subjects was then subjected to macroscopic qualitative examination to identify those portions of brain with the most dense collections of leptomeningeal melanin. These portions were sectioned and stained with hematoxylin-eosin as well as Prussian blue. The remaining brain tissue was not further studied. MR imaging and CT in these persons was performed as described for our normal imaging study, below.

Qualitative comparison was made of the gross specimens, stained sections, MR imaging, and CT. We in-

spected the leptomeninges shown on the CT and MR images for the previously reported imaging characteristics of intracranial melanin (5–7): on precontrast CT, normal to high attenuation compared with adjacent normal gray matter; on precontrast T1-weighted MR imaging, isointense to hyperintense compared with adjacent normal gray matter; and on T2-weighted MR imaging, isointense to hypointense compared with adjacent normal gray matter.

Normal Imaging Study

Using imaging records from the last 3 consecutive years, we selected all patients undergoing MR imaging focused on the posterior fossa. Clinical records on these patients were then reviewed. Patients were excluded if they had any of the following head, neck, or central nervous system conditions: hearing loss, neoplasm, infection, inflammation, trauma, neurofibromatosis, or surgery. MR imaging on this group was performed with a 1.5-T system (Signa, General Electric Medical Systems, Milwaukee, Wis) using a quadrature head coil. Spin-echo and/or fast spin-echo sequences were used to provide a study focused on the temporal bones and posterior fossa. These consisted of the following sequences: 4- to 5-mm-thick T1-weighted sagittal images, extending from one internal auditory canal to the other (500–600/10–20/1 [repetition time/echo time/excitations]) with a 256 × 128 matrix, 1-mm intersection gap, and 20-cm field of view; T2-weighted (2500–5000/30–100/1) 5-mm-thick axial images extending at least from the foramen of Monro through to the dens with a 1.0-mm intersection gap, 20-cm field of view, 256 × 256 matrix, and first-order flow compensation; and 3-mm-thick axial T1-weighted images (500–600/10–20/2) extending from the cavernous sinuses through to the hypoglossal foramina with a 0.5-mm intersection gap, 20-cm field of view, and 256 × 192 matrix. This axial sequence was performed before and immediately after the intravenous infusion of gadopentetate dimeglumine at 0.1 mmol/kg. Some patients also had postcontrast sagittal imaging, identical in technique to the precontrast sagittal sequence described above.

Some of these patients had also undergone temporal bone CT. The CT was performed either with or without intravenous contrast material on a General Electric 9800 unit; 1.5-mm-thick, 16-cm field-of-view images were obtained of the temporal bones and posterior fossa centered between the internal auditory canals. Although the entirety of the temporal bones was not always included, imaging from the cavernous sinuses through to the hypoglossal canals was uniformly done. Soft-tissue and bone algorithms were used.

The leptomeninges shown on these images were searched for the above-described imaging characteristics of intracranial melanin.

Results

Normal Anatomic Study

We found eight black subjects who had MR and CT focused on the posterior fossa within 12 months before the autopsy. Only two of these eight were found to have leptomeningeal melanin visible to the naked eye. The first was a 59-year-old man whose cause of death was sepsis. The second was a 79-year-old woman whose cause of death was pulmonary emboli. Macroscopically, leptomeningeal melanin appeared most dense in the leptomeninges surrounding the ventral portions of the medulla oblongata. There were no medulla oblongata abnormalities reported in the autopsy records. Review of our gross and sectioned autopsy material by a neuropathologist (M.B.) showed no medulla oblongata abnormalities. Prussian blue stain showed no iron in or around the medulla oblongata (Figs 1 and 2).

The histopathology of both subjects showed diffuse leptomeningeal melanin, most highly concentrated in the ventral leptomeninges of the medulla oblongata. This melanin was visible macroscopically, becoming more dramatic on stained section (Figs 1 and 2).

The indication for CT and MR imaging in both subjects had been suspected cerebellar degeneration and hearing loss. They did not receive contrast material for CT. CT and MR imaging showed cerebellar atrophy, but the medulla oblongata was normal in both.

The distribution of regions of mild to moderate hypointensity on T2-weighted images corresponded very well to the distribution of leptomeningeal melanin (compare Figs 1A with C and 2A with C). In both subjects, there was patchy high intensity in the leptomeninges of the medulla oblongata on T1-weighted precontrast images. The distribution of this high intensity corresponded poorly to the distribution of leptomeningeal melanin (compare Figs 1A with D and 2A with D). After gadopentetate dimeglumine, neither patient showed pathologic contrast enhancement in the leptomeninges.

CT demonstrated no convincing attenuation changes corresponding to the distribution of leptomeningeal melanin.

Normal Imaging Study

Our review of imaging and clinical records found 74 qualifying subjects with ages ranging

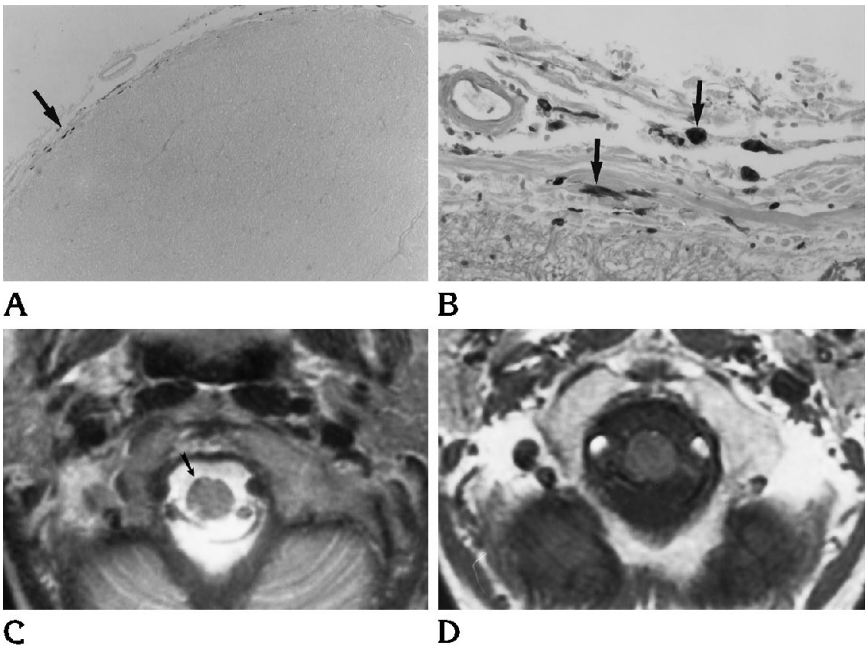

Fig 1. Histopathologic analysis and MR imaging of a 59-year-old black man from our normal anatomic study.

A, Microscopic section of the medulla oblongata stained with Prussian blue (magnification, × 5). Normal leptomeningeal melanin is visible as dark patches, with a notable cluster in one area (*arrow*).

B, Microscopic section of the medulla oblongata stained with hematoxylin-eosin (magnification, × 40). In this section, immediately contiguous with that shown in *A*, the cluster of dark melanin is dramatic; some is deposited in large focal collections (*arrows*).

C, Axial MR image (3000/90). Hypointensity is more marked along the ventral medulla than the dorsal medulla. A focus of more marked hypointensity (*arrow*) corresponds with the location of the dense leptomeningeal melanin collection shown on the histopathologic sections above. In this subject's histopathologic study, leptomeningeal melanin was most concentrated in this single area.

D, Axial MR image (566/15). The distribution of hyperintensity along the surface of the medulla corresponds poorly to the histopathologic distribution of leptomeningeal melanin.

from 15 to 78 years. Twenty-four of these 74 subjects had also undergone CT focused on the temporal bones and posterior fossa. Three of these 24 CTs were performed without intravenous contrast material; the remaining 21 were performed only with intravenous contrast material.

Thirty-one of the 74 patients were black. T2-weighted hypointensities similar to those seen in our normal anatomic study were seen in 28 of the 31 black patients. Both spin-echo and fast spin-echo T2-weighted sequences showed these signal changes.

The degree of hypointensity varied in these 28 subjects. Data in the clinical record were not adequate to assess the degree of skin pigmentation in each person. However, the subject with the most marked hypointensity (Fig 3A) had visited the dermatology clinic for keloid treatment 2 years before the MR imaging. The clinic record described him as "a naturalized African with very deeply pigmented skin."

Similar T2-weighted hypointensity was subtle, or entirely absent, in the remaining 46 subjects. This 46-subject group was made up of 3 black subjects and 43 nonblack subjects. Although subtle leptomeningeal hypointensity was seen in 6 of these 46 subjects, the remaining 40 had no such hypointensity. Clinical records were not adequate to evaluate the degree of skin pigmentation of all 6 subjects with subtle hypointensity. However, records in 5 of these 6 indicated that the patients were Asian, Middle Eastern, Pakistani, or Indian.

Faint, spotty, precontrast T1-weighted hyperintensity was seen in the leptomeninges of 18 of the 31 black subjects, and in 26 of the 43 nonblack subjects. The distribution of this T1-weighted hyperintensity corresponded poorly to the distribution of their T2-weighted hypointensity (compare Fig 3A with B).

Three of the 24 subjects undergoing CT were studied without intravenous contrast material. There were no precontrast attenuation changes along the surface of the medulla oblongata in these 3. No subject showed pathologic contrast enhancement.

Discussion

Normal intracranial melanin occurs only in two forms, neuromelanin and melanosomic melanin (2). In both forms, the melanin itself appears as granules. However, these granules are different on the ultrastructural level. Melanosomic or "true" melanin is the same type of melanin as that seen in the skin and iris of the eye. These melanin granules are confined to

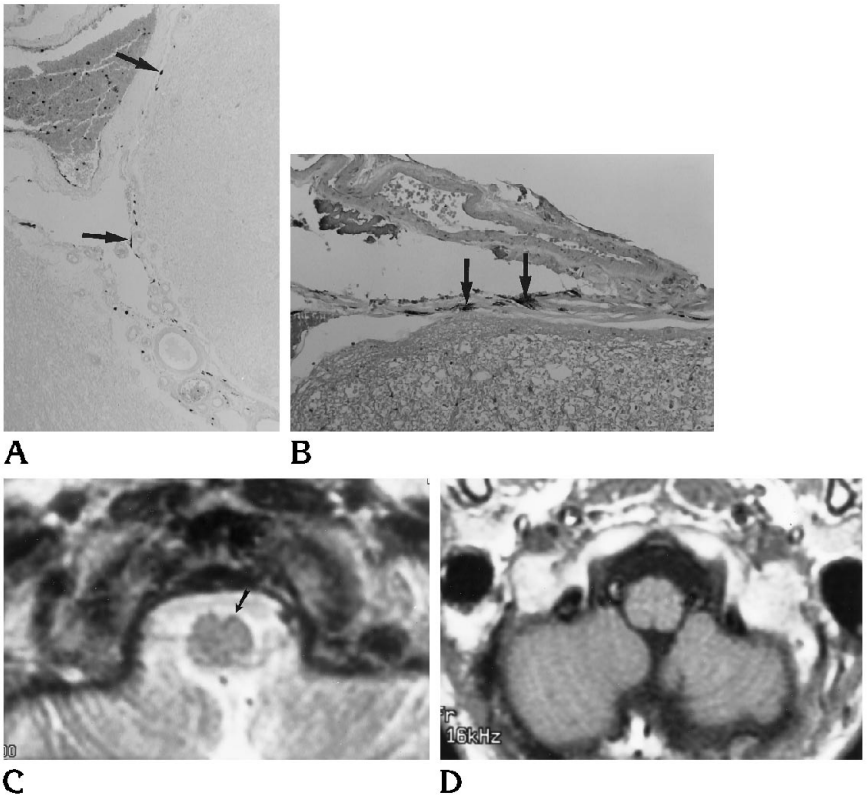

Fig 2. Histopathology and MR imaging of a 79-year-old black woman from our normal anatomic study.

A, Microscopic section of the medulla oblongata stained with Prussian blue (magnification, × 10). Normal leptomeningeal melanin is visible as dark patches, some fairly large (*arrows*). In this subject, these patches were distributed more densely along the left side of the ventral medulla oblongata than the right.

B, Microscopic section of the medulla oblongata stained with hematoxylin-eosin (magnification, × 20). This section is contiguous with the section displayed in *A* and shows a particularly dense collection of the dark melanin granules along the superior aspect of the left side of the ventral medulla (*arrows*).

C, Axial MR image (4000/100). Hypointensity is most marked on the ventral surface of the medulla oblongata, especially along the left side superiorly and medially (*arrow*). This distribution of hypointensity corresponds well to the histopathologic distribution of leptomeningeal melanin.

D, Axial MR image (600/11). No corresponding accentuation of hyperintensity along the ventral surface of the medulla.

melanosomes within melanocytes. Neuromelanin, on the other hand, presents as scattered intraneuronal inclusions of granular melanin not contained in melanosomes. The distribution of these two types of melanin is different. Neuromelanin is generally confined to certain groups of neurons including the zona compacta of the substantia nigra, locus ceruleus, dorsal motor nucleus of the vagus, tegmentum of the brain stem, and scattered neurons in the roof of the fourth ventricle. Melanosomic melanin is normally found only in the leptomeninges, where it is contained by melanocytes. These melanocytes are usually most concentrated in the leptomeninges over the ventral aspect of the medulla oblongata (1–4). In this location, the pigmentation is often visible macroscopically. As with all melanocytes, these cells are of neural crest origin, developing from normal melanoblasts (4).

Numerous intracranial pathologic entities contain melanin, the most common of which is metastatic melanoma (5). However, resident leptomeningeal melanocytes are believed to be responsible for the development of other less-common pathologic conditions such as neurocutaneous melanosis, meningeal melanocytoma, and primary meningeal melanoma (1, 3, 4, 7). The neoplastic nature of these three entities is agreed on, with neurocutaneous melanosis and meningeal melanoma behaving in a malignant fashion. Primary meningeal melanocytoma, a rare lesion, can be remarkably benign, as evidenced by clinical behavior and histologic features, including absence of necrosis and lack of mitotic activity (4, 7).

The normal and abnormal distribution of intracranial melanin is well known in the pathologic literature (1–4). However, the imaging literature is restricted to studies of neoplastic entities (5–7). Of all of the leptomeninges-based melanin-containing entities reported in the imaging literature, benign meningeal melanocytoma may be expected to show imaging characteristics most similar to normal leptomeningeal melanin.

In our normal anatomic study, we found that the distribution of T2-weighted hypointensity showed good correspondence to the histopathologic distribution of normal leptomeningeal melanin. This was supported by findings from our normal imaging study, which showed similar hypointensity in 28 of the 31 black subjects, but less convincing hypointensity, or no

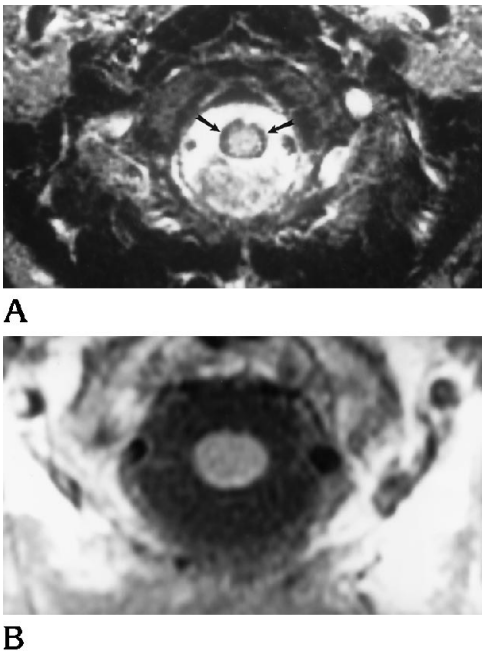

Fig 3. MR Imaging from a subject in our normal imaging study.

A, Axial MR image (4000/100). This was the most profound medulla oblongata hypointensity (*arrows*) that we found in our study. This subject has very deeply pigmented skin.

B, Axial MR image (566/11). Poor correspondence of the distribution of T1-weighted hyperintensity to the distribution of T2-weighted hypointensity.

such hypointensity, in the 43 nonblack subjects. In both our normal anatomic and our normal imaging studies, only faint, spotty, precontrast T1-weighted hyperintensity was seen. In our normal anatomic study, this hyperintensity corresponded poorly to the histopathologic distribution of normal leptomeningeal melanin. These findings suggest that the T2-weighted hypointensity is caused, at least in part, by normal leptomeningeal melanin, whereas the T1-weighted hyperintensity is probably caused by factors other than normal leptomeningeal melanin.

It has been shown that the paramagnetic effects of intracranial melanin are attributable to melanin itself, not complexes of melanin with iron or other paramagnetic ions (6). Though profound precontrast T1-weighted hyperintensity is known in intracranial nonhemorrhagic melanotic melanoma (5, 6), this hyperintensity is not a feature of meningeal melanocytoma (7). Meningeal melanocytoma has been reported to show precontrast T1-weighted signal, which is isointense compared with the adjacent medulla oblongata (7). Nonhemorrhagic metastatic melanotic melanoma shows an isointense to mildly hypointense appearance compared with normal brain on T2-weighted images (5, 6). But meningeal melanocytoma has been reported to show T2-weighted signal that is more frankly hypointense compared with the adjacent normal brain (7). The lack of preferential T2 shortening in metastatic melanomas has been explained by the presence of both intracellular and extracellular melanin, which could sufficiently reduce susceptibility gradients, thereby reducing the degree of T2 shortening (5). Normal leptomeningeal melanin is entirely contained within melanosomes, which are entirely contained by melanocytes. This storage pattern is similar to hemosiderin, which is mainly sequestered in macrophage lysosomes. Hemosiderin is known to cause preferential T2 shortening (5).

We found no CT attenuation alterations corresponding to the distribution of normal leptomeningeal melanin. Meningeal melanocytoma has been reported to show marked high attenuation (7), but the reported melanocytoma was a large mass. The relatively small amounts of normal leptomeningeal melanin are probably inadequate to change electron density enough to be demonstrated on routine CT.

We are mindful that some of the signal changes that we describe may be artifactual or attributable to materials other than leptomeningeal melanin. In fact, much of the T1-weighted hyperintensity is probably caused by a flow artifact from cerebrospinal fluid and the numerous small vessels in the leptomeninges around the medulla oblongata. Flow, magnetic susceptibility, and chemical-shift artifacts may play a role in the generation of the T2-weighted hypointensities along the surface of the medulla oblongata in our patients. Fast spin-echo sequences, lower-field-strength MR units, and shorter-repetition-time spin-echo sequences would be expected to be less sensitive to magnetic susceptibility effects than conventional long-repetition-time spin-echo sequences (11). However, on our 1.5-T long-repetition-time images, we found hypointensity around the medulla oblongata on both conventional spin-echo (Fig 1C) and fast spin-echo (Figs 2C and 3A) T2-weighted sequences. Signal changes similar to ours have been reported from intracranial iron (6). Prussian blue–stained sections of our specimens showed no iron (Figs 1A and 2A).

Some of our subjects demonstrated quite frank T2-weighted hypointensities (Figs 1C and 2C), with one subject showing profound hypointensity (Fig 3A). Such profound signal alterations from normal leptomeningeal melanin could simulate diffuse leptomeningeal diseases that contain melanin or iron, especially leptomeningeal melanosis or siderosis (11). Fortunately, the leptomeningeal T2-weighted hypointensity of melanosis or siderosis is usually thicker and more extensive than that of normal leptomeningeal melanin, and siderosis is often caused by a known prior intracranial hemorrhage, many times a hemorrhagic ependymoma (11). If a question does arise, however, correlation with the degree of skin pigmentation in the subject, and the absence of any other pathologic leptomeningeal MR imaging characteristic, should resolve the issue. MR imaging findings in all other leptomeningeal diseases, such as inflammation, infection, or metastatic neoplasm, can usually be differentiated from the signal changes of normal leptomeningeal melanin. This is because these other leptomeningeal diseases almost always result in pathologic contrast enhancement, thickening, nodularity, or even frank mass, none of which were present in our subjects (8–11).

Normal leptomeningeal melanin is visible on MR imaging as T2-weighted hypointensities along the surface of the medulla oblongata. The signal changes from this pigment are often subtle but can be dramatic. The potential for signal alterations caused by normal leptomeningeal melanin should be taken into account before diagnosing abnormalities in this region.

References

1. Burger PC, Scheithauer BW, Vogel FS. *Surgical Pathology of the Nervous System and Its Coverings*. 3rd ed. New York: Churchill Livingstone, 1991:115–117
2. Hirano A. Neurons and astrocytes. In: Davis RL, Robertson DM, eds. *Textbook of Neuropathology*. 2nd ed. Baltimore: Williams & Wilkins, 1991:15–18
3. Norman MG, Ludwin SK. Congenital malformations of the nervous system. In: Davis RL, Robertson DM, eds. *Textbook of Neuropathology*. 2nd ed. Baltimore: Williams & Wilkins, 1991:272–273
4. Russell DS, Rubinstein LJ. *Pathology of Tumors of the Nervous System*. 5th ed. Baltimore: Williams & Wilkins, 1989:792–797
5. Atlas SW, Grossman RI, Gomori JM, et al. MR imaging of intracranial metastatic melanoma. *J Comput Assist Tomogr* 1987;11:577–582
6. Atlas SW, Braffman BH, LoBrutto R, Elder DE, Herlyn D. Human malignant melanomas with varying degrees of melanin content in nude mice: MR imaging, histopathology, and electron paramagnetic resonance. *J Comput Assist Tomogr* 1990;14:547–554
7. Naul LG, Hise JH, Bauserman SC, Todd FD. CT and MR of meningeal melanocytoma. *AJNR Am J Neuroradiol* 1991;12:315–316
8. Burke JW, Podrasky AE, Bradley WG Jr. Meninges: benign postoperative enhancement on MR images. *Radiology* 1990;174:99–102
9. Chang KH, Han MH, Roh JK, Kim IO, Han MC, Kim C-W. Gd-DTPA-enhanced MR imaging of the brain in patients with meningitis: comparison with CT. *AJNR Am J Neuroradiol* 1990;11:69–76
10. Paakko E, Patronas NJ, Schellinger D. Meningeal Gd-DTPA enhancement in patients with malignancies. *J Comput Assist Tomogr* 1990;14:542–546
11. Sze G. Diseases of the intracranial meninges: MR imaging features. *AJR Am J Roentgenol* 1993;160:727–733